Polichromatic Image Sensor With Microlenses For Stereoscopic Acquisition

R. P. Rocha, J. P. Carmo, M. F. Silva, J. H. Correia
Department of Industrial Electronics
University of Minho
Guimarães, Portugal
rrocha@dei.uminho.pt

***Abstract*—This paper presents the fabrication of microlenses for integration on a stereoscopic image sensor in CMOS technology and a low-cost technology for fabricating optical filters arrays tuned for the primary colors. The material selected for fabricating the microlens was the AZ4562 positive photoresist and the fabrication process explained. Moreover, the fabrication process presented in this paper is for directly printing the optical filters into a transparent flexible substrate (acetate).**

Keywords; Microlenses, optical filters, RGB, image sensor, stereoscopic vision, low-cost fabrication.

I. INTRODUCTION

Currently, the available image sensing technology is not yet ready for stereoscopic acquisition. The final quality of the image will be improved because of the stereoscopic vision but also due to the system's high resolution. Typically, two cameras are used to achieve a two points of view (POV) perspective effect. But this solution presents some problems mainly because the two POVs, being sufficiently different, cause the induction of psycho-visual confusion by the user [1]. The parallax effect, illustrated in Figure 1, is used to achieve stereoscopic vision. The result is obtained by "tricking" the brain causing it to gain depth perception (also known as stereopsis). This means that bad quality stereoscopy induces perceptual ambiguity in the viewer [2]. The reason for this phenomenon is that the human brain is simultaneously more sensitive but less tolerant to corrupt stereo images as well as vertical shifts of both images, being more tolerant to monoscopic images. Therefore, the brain does not consent the differences between the images coming from the left and right channels that are originated from the two independent and optically unadjusted cameras. Furthermore, the outspread of low-power small dimensioned high-resolution cameras motivates even more the fabrication of the next generation of such devices. Another advantage of the proposed imaging sensor is the compatibility with the CMOS technology.

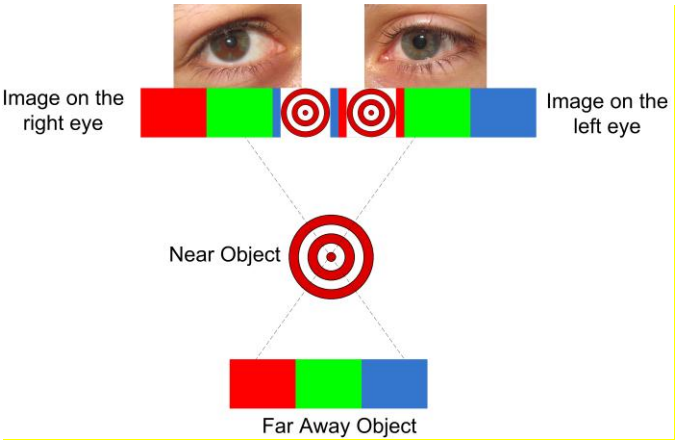

Figure 1: Illustration of the parallax effect for inducing sensation of depth in the human brain [1].

Most notably, CMOS allows the decrease of the power consumption and, unlike the CCD technology, CMOS sensors can be fabricated using the same manufacturing facilities as the high-volume products of the semiconductor industry. Thus, CMOS microdevices are more standardized and cost-effective to produce then the CCD microdevices. Considering the low-power consumption of the CMOS microdevices, another possibility that presents itself for the imaging sensors is the integration of thin-films batteries with silicon compatibility [3] and low toxicity [4]. The fabrication of such a microdevice can be done using the 0.7 µm CMOS process in the AMIS foundry because it allows the production of both the photodetectors and the read-out electronics within a reasonable cost. Finally, since the aforementioned process is very well characterized and known, the time to manufacture the first working prototype is expected to be short. This paper addresses on the design and fabrication technology of the microlenses for providing stereoscopic vision.

II. IMAGE SENSOR ARCHITECTURE

The image sensor is composed by two pupils (two entrance apertures just like the human eyes) from where the left and right channels (the two POVs that will originate the tridimensional effect) pass through before being focused by an objective lens. This lens focuses the two incident beams in the direction of the microlens, where the light is concentrated in a

small sensitive area where the photodiodes are placed. After passing through the optical filters, the wavelengths coming from both the entrance apertures are directed towards the respective CMOS photodiodes. The two viewpoints are separated by focusing each side onto the appropriate sensor column under the microlens and optical filters.

III. SENSOR FABRICATION

A. *The structures of the stereoscopic image sensor*

The photodetector is a n+/p-epilayer junction photodiode fabricated in a CMOS process, because it provides the best possible quantum efficiency in the desired spectral range of photodiodes available in a CMOS process. Moreover it yields the highest possible fill-factor, since a deep n-well is not required for every pixel [5]. In the 0.7 µm selected CMOS process, the junction depth of the photodiodes is fully defined and cannot be altered. However, the quantum efficiency can be improved by a suitable arrangement of dielectric layers on top of the photodiode surface. These act as a thin-film interference filter and influence the optical transmittance for each wavelength independent of the CMOS process. In this CMOS process there are three major dielectric layers above the photodiode p-n junction. The first oxide (boron phosphor silicate glass is the metal1-poly oxide) is above the photodiode. The second major oxide comprises those between the first and second metal layers. The last layer (overlayer) is made of silicon nitride. In the literature it can be found that a photodiode structure without two of the three dielectric layers above the pn-junction will provide the best quantum efficiency in the desired spectral range in a CMOS process [6].

B. *Optical filter fabrication*

The thin-film deposition of a material in a carrier substrate (glass or quartz) is the common method to fabricate optical filters. Normally, the fabrication of thin-films with a band-pass around a given wavelength is done by successively depositing different dielectric materials in order to obtain a dielectric multilayer structure able to achieve that characteristic. For each primary color, the thin-films are designed to yield a given band-pass around the respective wavelengths. However, the fabrication of optical filters based on thin-films made of dielectric materials is complicated (in spite of well-tuned and characterized) with a high number of process steps and thus, increased fabrication costs. The method proposed in this paper for fabricating optical filters can be implemented with low-cost because a standard color printer (with the suitable resolution) and a sheet of acetate (the substrate) is the only required equipment. The details and results about the fabrication of the optical filters will be presented in the next section.

C. *Microlenses*

Several different materials are available for fabricating microlenses. Some of these candidate materials can be selected, e.g., SU-8/2, AZ9260 and AZ4562. These photoresists (PR) allow the fabrication of microlenses by thermally reflowing the raw material. This allows the production of arrays containing the microlenses with a high degree of reproducibility of their characteristics.

IV. EXPERIMENTAL

A. *Microlenses FEM simulations*

In Figure 2 it is possible to see the results of some finite element method (FEM) simulations.

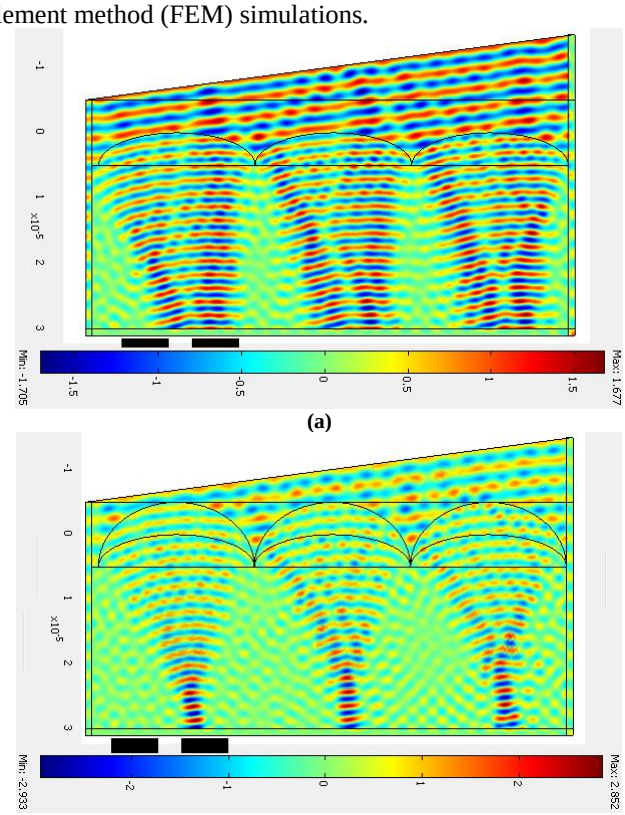

(a)

(b)

Figure 2: FEM simulations showing the light concentration into the right photodiode. The simulations where obtained respectively for lenses measuring with (a) W/L=4.8 and (b) W/L=2.4. The simulations also allows to roughly estimate the degree of cross talk between two adjacent photodiodes (e.g., between the left and right channels).

These simulations were performed considering the impinging light with an angle of 7.6º degrees from the left channel, but this methodology is also applicable to the right channel and both channels overlapping for the global effect. The dimensions of the presented microlenses simulations have a W/L ratio of 4.8 and 2.4 in (a) and (b), respectively. It is clearly seen that the light concentrates in the direction of the photodiodes represented as pairs of black rectangles on the bottom of the figure. The simulations also show that the best results, *i.e.* more concentration of light, are achieved with microlenses having a higher curvature. Moreover, another important conclusion is shown, that it is possible to separate the left and right channels for focusing the specific wavelengths into the respective photodiodes. This also allows estimating the cross-talk between adjacent photodiodes, being smaller in the micro lenses with higher curvature. It is assumed in the simulations that the light had already passed through the optical filters.

B. *Microlenses fabrication*

The photoresists used allow the microlenses fabrication by

thermally reflowing the raw material, whose processing steps are presented in Figure 3.

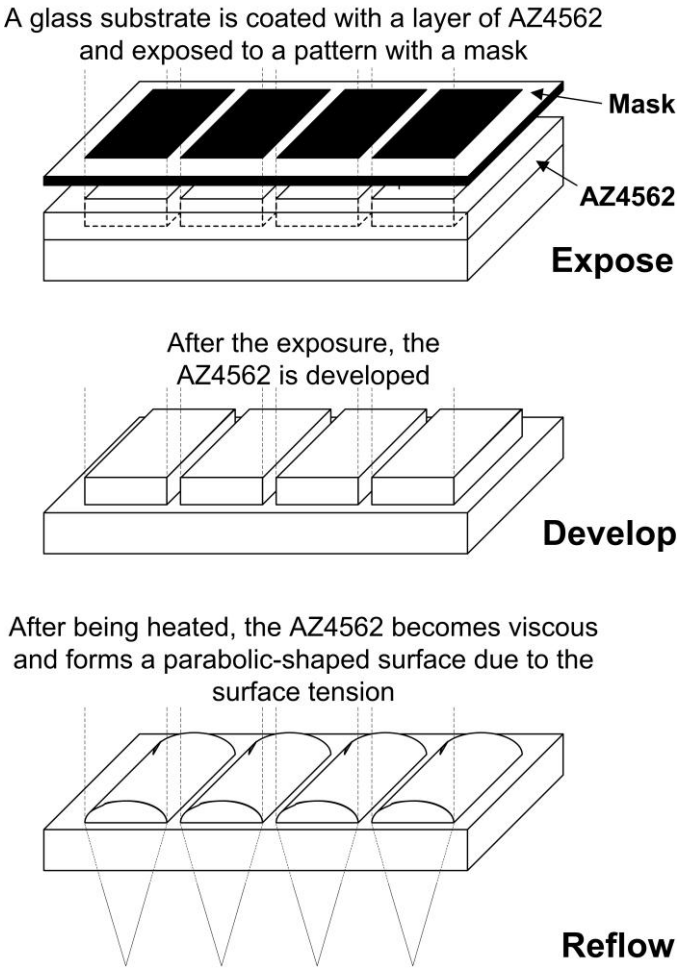

Figure 3: The reflow process applied to the AZ4562 photoresist for fabricating microlenses arrays.

The fabrication process of the microlenses array is as follows: First, it is necessary to deposit the photoresist by means of a spin coater. After the coating, a prebake phase, using a computer controlled hot plate is necessary to evaporate the solvent present in the photoresist. This step is critical otherwise the resist surface dries very fast and doesn't allow the solvent to exit the photoresist creating bubbles and possibly the photoresist to lift. Next, to obtain the required array-like structure, the mask with the correspondent geometrical design is placed on top of the substrate with the photoresist for exposing the PR to UV light, making the unexposed material insoluble. Afterwards, the development phase, is required to leave just the unexposed photoresist in the substrate. Finally, in order to obtain the lenses profile, a reflow technique is used by heating up the substrate in a hotplate.

C. Characterization

In Figure 4, two photographs show the PR array before and after the reflow step, respectively, on the left, top view and on the right, tilted view. The tilted view photo taken using an optical microscope is focusing only in the curved edge of the array.

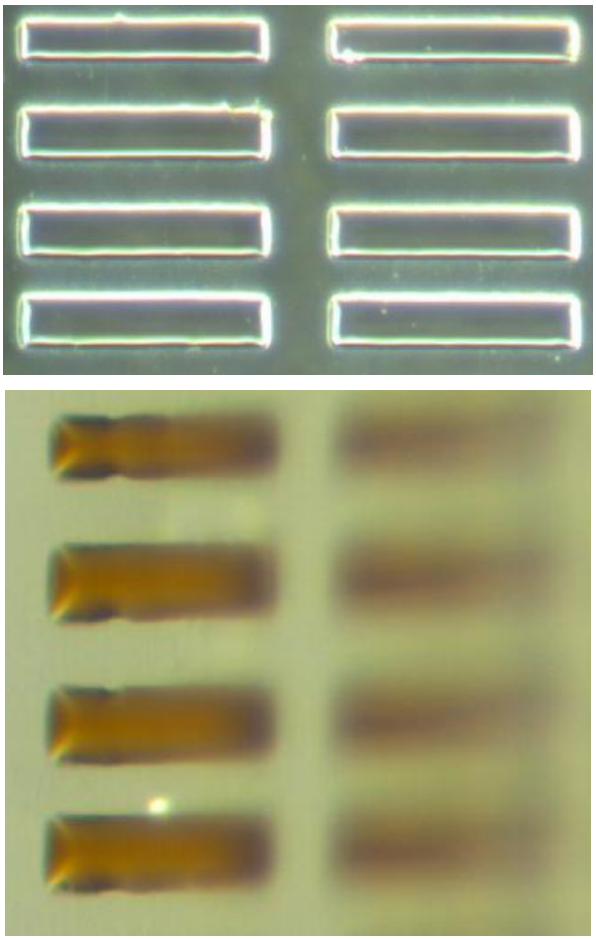

Figure 4: The photoresist array before and after the reflow, on the top and bottom, respectively.

In Figures 5 (a) and (b) it is possible to see the profiles of the PR before and after the reflow process measured with a Veeco Dektak 150 profilometer.

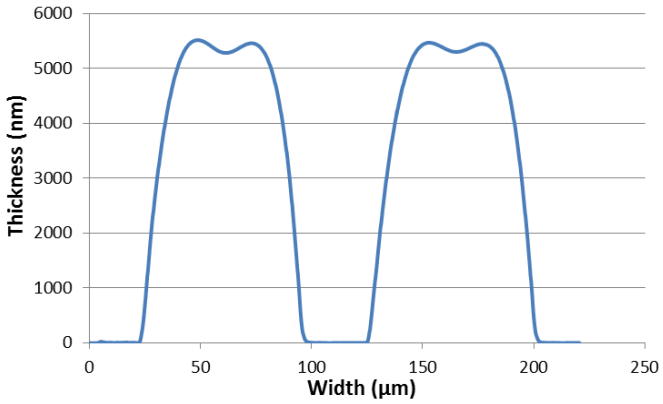

Figure 5: (a) – Profile of the PR array before the thermal reflow.

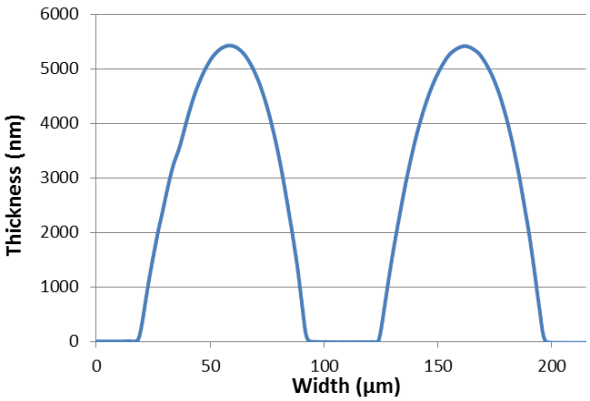

Figure 5: (b) Profile of the microlenses obtained after the thermal reflow step.

This figure presents the typical initial profile seen during the fabrication of microlenses using PR [7,8]. After applying a temperature higher than the glass transition temperature of the PR, the viscosity decreases and the consequent flow due to surface tension occurs. These structures are the first prototypes built using photolithography but the final size of the microlenses can be further reduced using a chromium-on-glass mask. Nevertheless, it is clear from the previous figures that the thermal reflow process permitted obtaining the desired microlens profile to concentrate the light into specific directions.

D. Optical filters

An array of RGB band-pass filters can be easily printed, when allowed by the printing process resolution. There are available in the market printers that allow the fabrication of optical filters with single cells of very low dimensions (with a minimum resolution of 20 µm), but their prices easily surpasses 60 k€. Despite the high cost that is initially imposed, it is expected a decrease in the cost per fabricated unit. At the current phase, the process to obtain filters was tested and characterized. Figure 6 illustrates the selected colors for fabricating individual optical filters. After the fabrication of these optical filters by printing them into an acetate sheet, the measurements were done as follows: a monochromator was used to scan individual wavelengths along the visible spectrum and, at the same time, a spectrometer measured the optical power. This procedure allowed to measurement of the optical transmittance of individual optical filters.

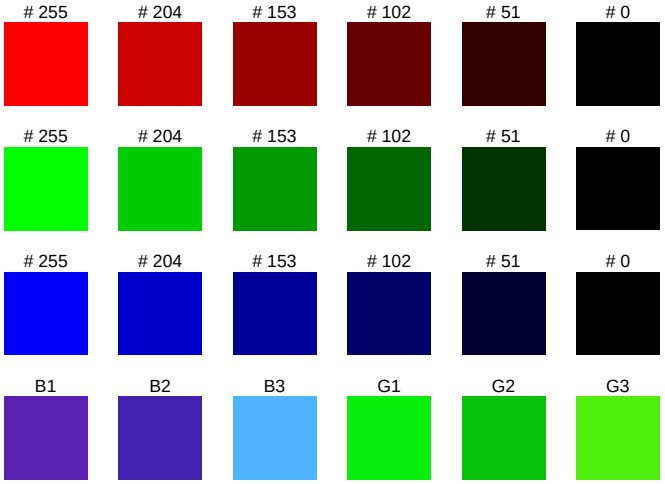

Figure 6: The used colors for fabricating the individual optical filters for further selection of the most suitable as candidate filters (those on Table I).

For the candidate filters that were selected among those with the highest potential for use in the image sensor, Table I shows their color fillings and the respective spectral measurements: the central wavelength, λ_0 [nm], and the respective full-width half-maximum, *FWHM* [nm]. As it can be observed, the most suitable set of optical filters is the one that contains the B1, G3 and R3. This is the set that simultaneously ensures better visible band coverage and minimizes the overlap between the adjacent RGB bands.

TABLE I. FEW PRINTED RGB OPTICAL FILTERS FOR MEASURING.

Color display	Filter	RGB level [%]	λ_0 [nm]	*FWHM* [nm]
	#1 (B1)	35.3-12.5-69.0	455	120
	#2 (B2)	25.1-13.3-68.2	462	121
	#3 (B3)	30.9-70.6-100	483	101
	#1 (G1)	3.1-93.3-5.1	525	78
	#2 (G2)	2.7-75.7-4.3	525	76
	#3 (G3)	31.4-93.3-5.1	525	95
	#1 (R1)	40-0-0	NA	NA
	#2 (R2)	60-0-0	NA	NA
	#3 (R3)	100-0-0	NA	NA

Figure 7 shows the band-pass spectra of the three selected filters (blue, green and red) taking into account the absolute amplitudes of the respective transmittances. This figure helps to understand why the B1, G3 and R3 filters were selected. Few further improvements must be done with respect to the green region of the visible spectrum because even with the best optical filter (G3), it remains a slight overlap with the red region of R3 (with relative amplitude of 50%). The overlap between the blue (B1) and green (G3) is less important due to the fast decrease of both plots when within the adjacent region.

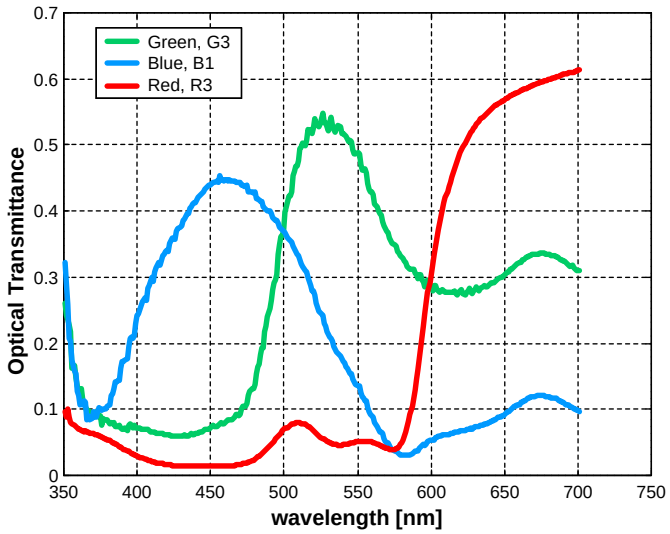

Figure 7: Amplitude spectra of the RGB filters (B1, G3 and R3) that were selected for fabricating the optical filtering prototype to use in the optical sensor.

In Figure 8 it can be seen the fabricated prototype of the optical filters built in an acetate sheet.

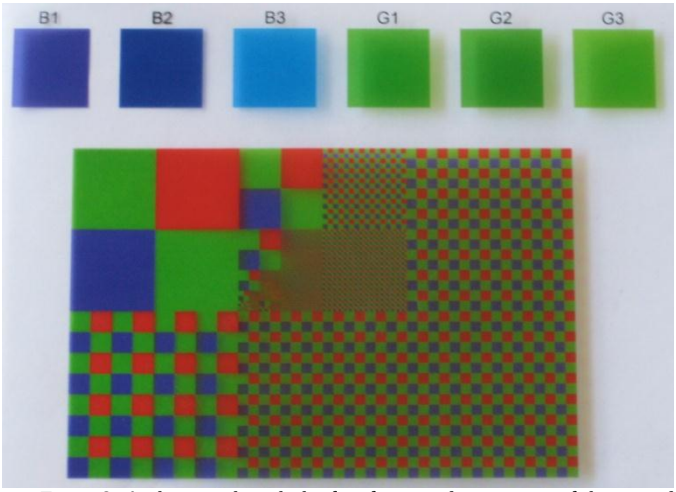

Figure 8: A photograph with the few functional prototypes of the optical filters listed in Table I.

V. CONCLUSIONS

This paper presented a microlenses fabrication process for integration on a stereoscopic image sensor in CMOS technology with high resolution. The main contributions are proposing a fabrication technology of arrays of microlenses and RGB optical filters at low-cost with the help standard photolithography processes and of a laser printing into a flexible and transparent substrate (e.g., acetate). The microlenses design started with the FEM simulations to set some parameters needed to fulfill the desired objectives. These objectives included the microlenses' W/L dimensional ratio of 4.8 and 2.4 because of the size and pitch of the photodetectors. Each photodetector measures a specific wavelength which is difracted by the microlenses. The complete fabrication process was explained and the initial and final structures obtained were physically characterized. It was shown that the reflow step is what determines the actual microlenses profile. The several steps that comprise the photolithographic fabrication process were done for a first prototype but smaller ones are already being developed and tested using a chromium-on-glass mask and a mask aligner as the UV light source. The photograph of the functional prototypes showed in Figure 8 confirms the possibility of getting large arrays of optical filters. For such purpose, the fabrication process must be the same based on direct color printing into acetate using an ordinary laser printer. Despite the interesting results that were obtained, further improvements must be done because the reflectivity of the impinging light is high in the border formed by the air and the surface of the filter. The next step will be the investigation of alternative substrates with better optical properties (with respect to reflectivity) and/or the investigation of coating materials for use as adaptation layer for reducing the reflectivity of the impinging light. Nonetheless, the experimental results revealed to be promising with respect to obtain suitable spectral transmittances. Also for future work, the fabrication of thin films with a band-pass around a given wavelength is done by successively depositing different dielectric materials in order to obtain a dielectric multilayer structure. For each primary color, the thin films yield a band-pass around the respective wavelengths. The dielectric materials contained in the optical filters are composed by a stack of TiO_2 and SiO_2 thin films (refractive indexes in the visible spectrum: around 3.0 and 1.5, respectively).

ACKNOWLEDGMENT

This work was fully supported by the Portuguese Foundation for Science and Technology under the project FCT/PTDC/EEA-ELC/109936/2009 and R. P. Rocha is supported by the Foundation for Science and Technology financial grant SFRH/BD/33733/2009.

REFERENCES

[1] I. Andorko, P. Corcoran, P. Bigioi, "Hardware implementation of a real-time 3D video acquisition system", in proc. of 12th International Conference on Optimization of Electrical and Electronic Equipment (OPTIM 2010), Brasov, Romania, 20-22 May, pp. 920-925.

[2] S. Zeki, "The neurology of ambiguity", Consciousness and Cognition, Vol. 13, pp. 173-196, 2004.

[3] C. K. Chan, *et al*, "High-performance lithium battery anodes using silicon nanowires", Nature, Vol. 3, pp. 31-35, January 2008.

[4] M. Armand, J.-M. Tarascon, "Building better batteries", Nature, Vol. 451, pp. 652-657, February 2008.

[5] J. P. Carmo, R. P. Rocha, M. F. Silva, D. S. Ferreira, J. F. Ribeiro, and J. H. Correia, "Stereoscopic image sensor with low-cost RGB filters tunned for the visible range", 18th IEEE International Conference on Electronics, Circuits and Systems (ICECS), 2011 Beirut, Lebanon, pp. 285-288, 2011.

[6] G. Minas, G. Graaf, R. Wolffenbuttel and J. H. Correia, "An MCM-based microsystem for colorimetric detection of biomolecules in biological fluids", IEEE Sensors Journal, Vol. 6, No. 4, pp. 1003-1009, August 2006.

[7] A. Emadi, H. Wu, S. Grabarnik, G. Graaf, and R. Wolffenbuttel, "Vertically tapered layers for optical applications fabricated using resist reflow", Journal of Micromechanics and Microengineering, 19, 2009.

[8] F. O'Neill and J. Sheridan, "Photoresist reflow method of microlens production Part I: Background and experiments", Optik 113, No. 9, pp. 391-404, 2002.